Electronic Supplementary Information

Water-resistant, strong, degradable and recyclable rosin-grafted cellulose composite paper

Penghao Sun,[†a] Siheng Wang,[†b] Zhen Huang,[a] Lei Zhang,[b] Fuhao Dong,[a] Xu Xu *[a] and He Liu *[b]

[a] Jiangsu Co-Innovation Center of Efficient Processing and Utilization of Forest Resources, College of Chemical Engineering, Nanjing Forestry University, Nanjing 210037, Jiangsu Province, China.

[b] Institute of Chemical Industry of Forestry Products, Chinese Academy of Forestry, Key Laboratory of Biomass Energy and Material, Key Lab. of Chemical Engineering of Forest Products, National Forestry and Grassland Administration, National Engineering Laboratory for Biomass Chemical Utilization, Nanjing 210042, Jiangsu Province, China.

† These authors contributed equally to this work.

* Corresponding authors. Email: xuxu200121@hotmail.com (X. X.), liuhe.caf@gmail.com (H. L.)

Contents

Figure S1. The FTIR of FHR, KH-561 and RM.……S4

Figure S2. The ^{1}H NMR of RM.……S5

Figure S3. Photograph of RM emulsion.……...S6

Figure S4. Particle size distribution of RM emulsion.…….……..…...S6

Figure S5. BET analysis of EP paper, RM paper-10 and RM paper-20…….……...S6

Figure S6. Surface morphology and WCA of RM paper……...S7

Figure S7. EDS mappings of EP paper. …….……S7

Figure S8. EDS mappings of RM paper-20. …….……S8

Figure S9. Si 2p XPS spectra of RM paper-20. ……..…S8

Figure S10. Photograph of EP paper and RM paper after soaking for 1 h.…….S8

Figure S11. Test of long-time water resistance of EP paper and RM paper……..…S9

Figure S12. Water-resistant test of KH-561 grafted cellulose paper……..S9

Figure S13. WCA of RM paper after wear…….……..S10

Figure S14. SEM images of RM paper after wear. …….S10

Figure S15. Acid and alkali resistance of RM paper……S11

Figure S16. Printability of RM paper-20 and EP paper.……..…S11

Figure S17. Water absorption of highly cross-linked polymers formed by RM polymerization ……...……...……..... S12

Figure S18. Thermal stabilit.…….....S12

Figure S19. Mechanical properties of RM paper after soaking in acid and alkali solution……S13

Figure S20. Water resistance and mechanical properties of RM paper-30 and RM paper-50 ……S13

Figure S21. Mechanical properties of KH-561 grafted cellulose paper……..S14

Figure S22. Mechanical properties of EP paper. ……...…….……S14

Figure S23. Mechanical properties of RM paper-20 straw after soaking for 240 min....S14

Figure S24. RM paper-20 straws are soaked in different drinks. …….……S15

Figure S25. The weight loss curve of different straws. ……..…S15

Figure S26. Water absorption of EP paper and R-EP paper. …….…….……S15

Figure S27. Tensile strength of EP paper and R-EP paper. ……..…S16
Table S1. Performance comparison……..…S16

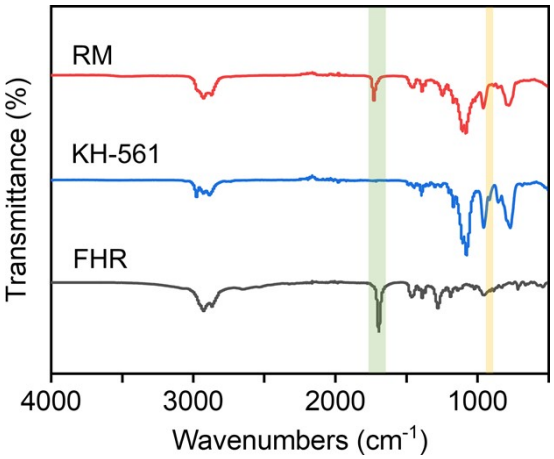

Figure S1. The FTIR of FHR, KH-561 and RM.

FTIR analysis

The absorption peak of epoxy group and Si-O-C in KH-561 can be observed at 910 cm^{-1} and 957 cm^{-1}, respectively.[1] After ring opening reaction, the absorption peak of epoxy group disappears (yellow part of picture) and the absorption peak of Si-O-C appears in the spectrum of RM. In addition, a wide absorption peak of -OH appears at 3420cm^{-1}.[2] Compared with FHR, the peak of C=O stretching vibration in RM spectrum shifted from 1690 to 1720 cm^{-1} (green part of picture) due to the formation of ester group.[3] The above results show that RM is successfully prepared.

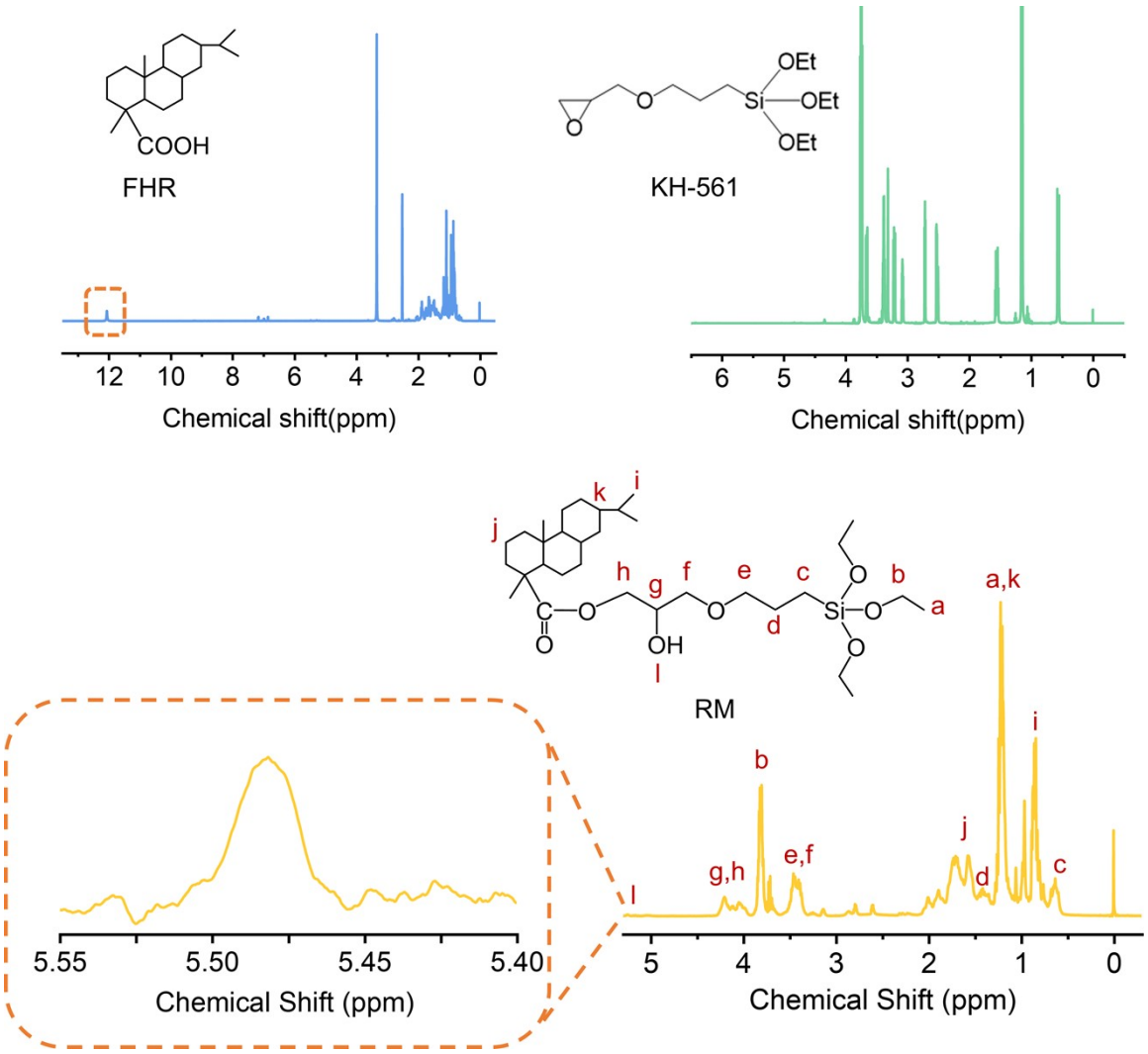

Figure S2. The ^{1}H NMR of FHR, KH-561, and RM.

^{1}H NMR analysis

The peaks of chemical shifts at 1.21 (attributed to -CH_3 in ethoxy) and 3.83 ppm (attributed to -CH_2- in ethoxy) can be clearly observed. Meanwhile, the peak of chemical shifts at 0.62, 1.42, 3.4 and 4.2 ppm are assigned to hydrogen on the -CH_2- of the alkyl chain in the KH-561. The peaks of chemical shifts from 1.2 to 2 ppm are attributed to hydrogen on FHR. The peak of chemical shift at 12.08 ppm is assigned to hydrogen on the carboxyl group of FHR. It is worth noting that the peak of chemical shift at 12.08 ppm disappears in the ^{1}H NMR of RM. Meanwhile, the peak of chemical shift at 5.48 ppm, which is attributed to the hydrogen on the hydroxyl group produced by ring opening reaction. The above results can further prove the successful preparation of RM.

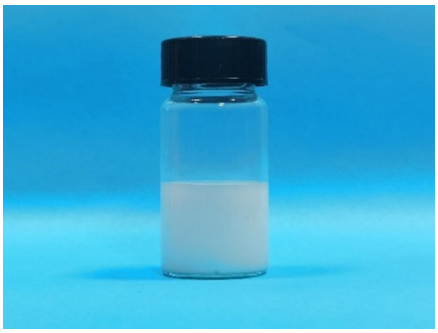

Figure S3. Photograph of RM emulsion. Cationic starch makes RM emulsion positively charged, which is not only conducive to maintaining emulsion stability, but also conducive to the adsorption of RM on cellulose fibers.

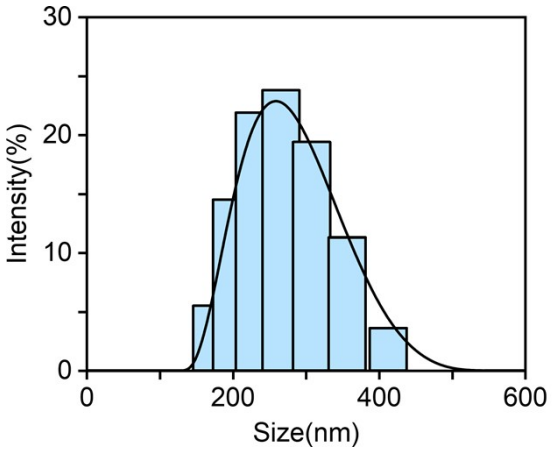

Figure S4. Particle size distribution of RM emulsion. The average particle size of RM emulsion is 265.6 nm.

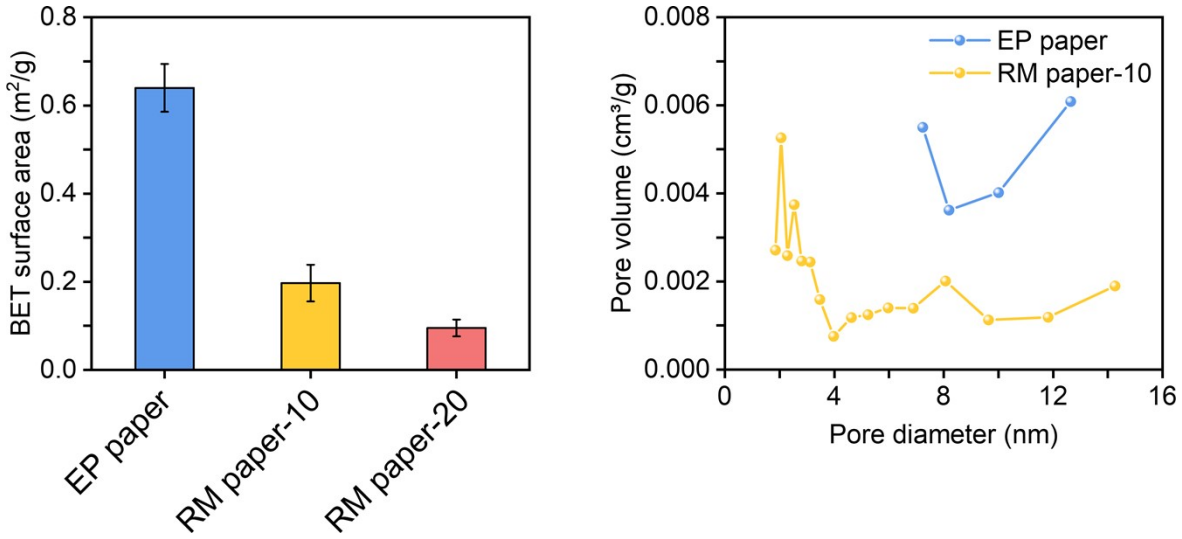

Figure S5. BET analysis of EP paper, RM paper-10 and RM paper-20.

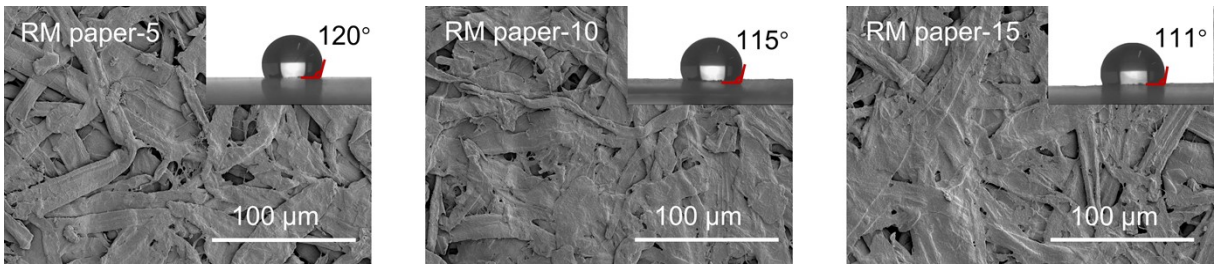

Figure S6. Surface morphology and WCA of RM paper-5, RM paper-10 and RM paper-15. With the increase of RM content, the structure of RM paper becomes denser and its surface becomes smoother, resulting in a slight decrease of WCA.

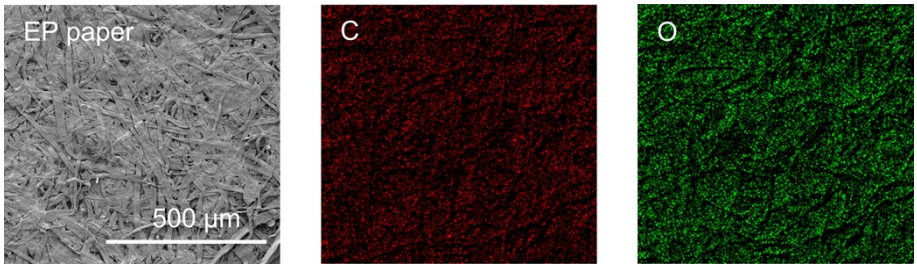

Figure S7. EDS mappings of EP paper. EP paper is made up of cellulose with only C and O elements on its surface.

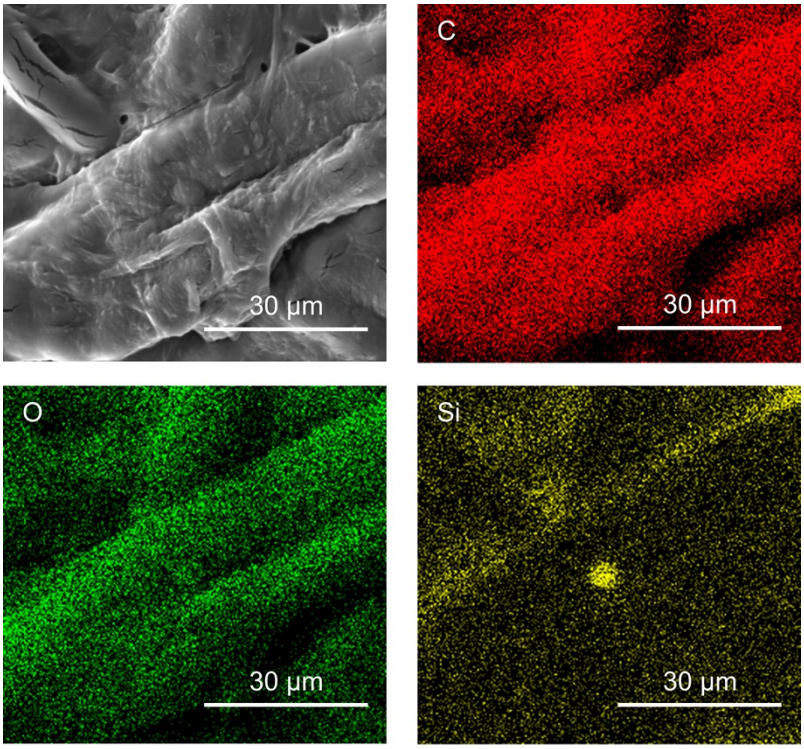

Figure S8. EDS mappings of RM paper-20. Si elements are distributed along the cellulose fibers and obviously accumulated in the micropores between the fibers, which indicated that the content of RM in the micropores increased. This phenomenon is attributed to the plugging of micropores by highly cross-linked polymers produced by RM polymerization.

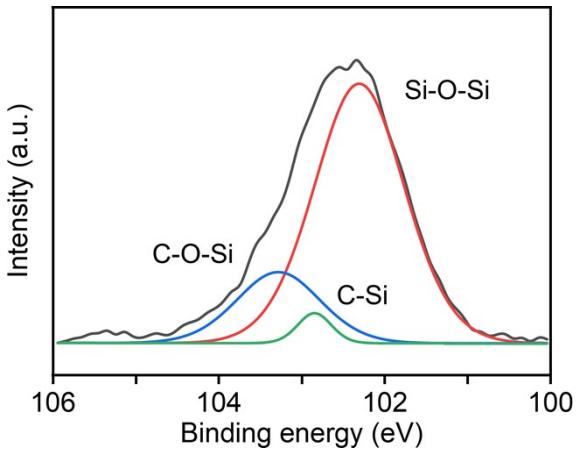

Figure S9. Si 2p XPS spectra of RM paper-20. Analysis of the spectra showed that the content of Si-O-Si bond accounts for the largest proportion, which confirms the polymerization of RM.

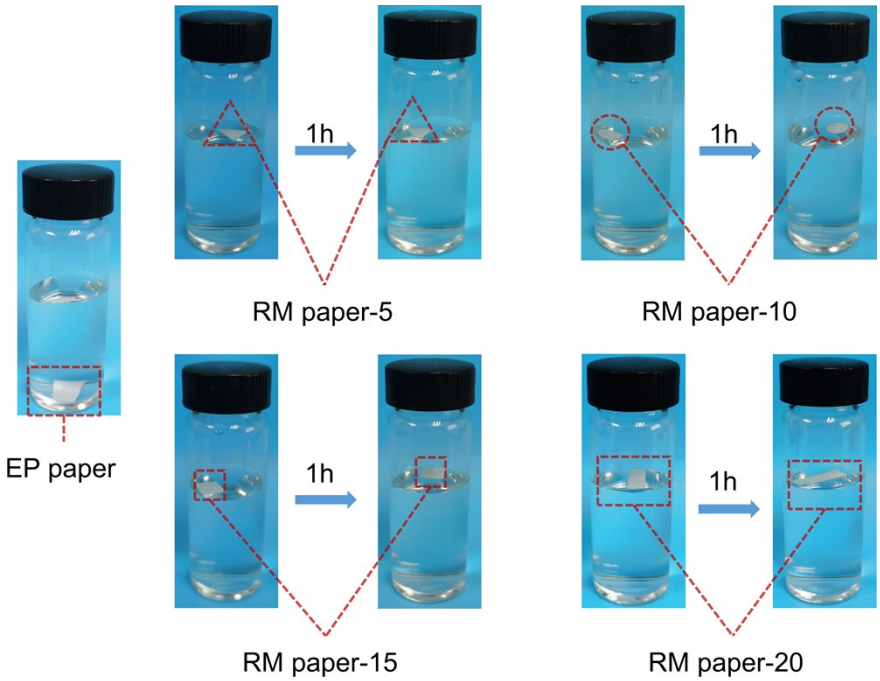

Figure S10. Photograph of EP paper and RM paper after soaking for 1 h. The high polarity of cellulose makes EP paper very sensitive to water, while RM paper remains stable in water due to the low polarity of hydrogenated phenanthrene ring.

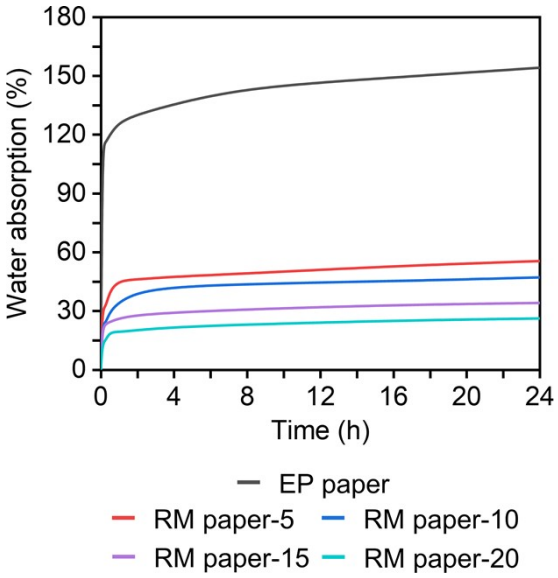

Figure S11. Test of long-time water resistance of EP paper and RM paper. Even after soaking in water for 24 h, RM paper still maintains excellent water resistance.

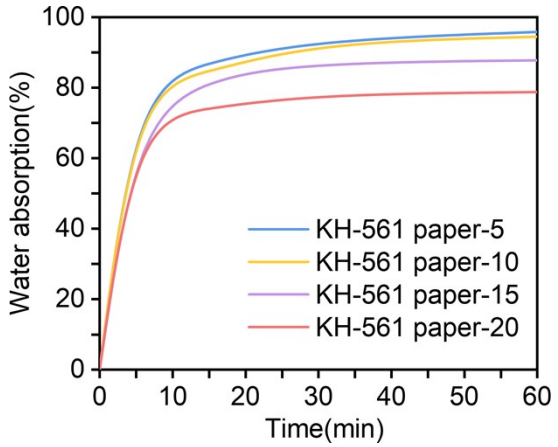

Figure S12. Water-resistant test of KH-561 grafted cellulose paper.

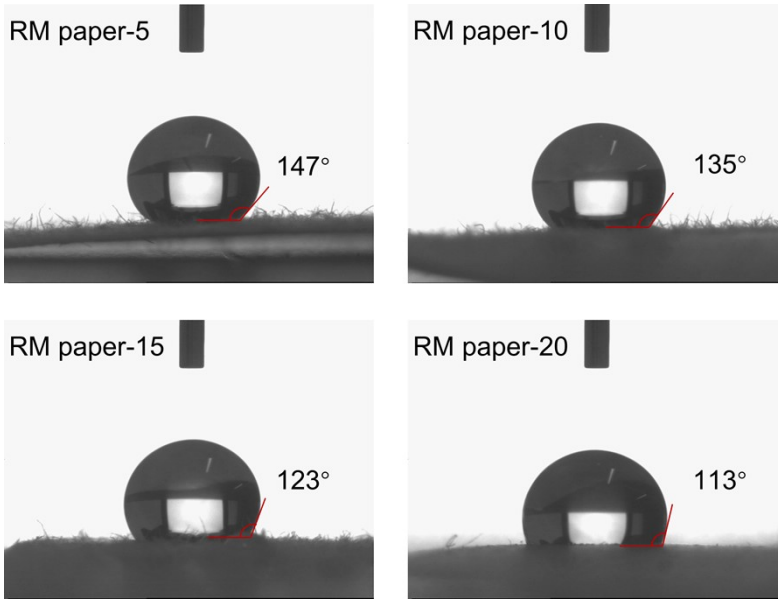

Figure S13. WCA of RM paper after wear. Wear causes the fibers to be destroyed, and the fine fibers on the surface expand the contact area between water and RM paper, which leads to the increase of WCA.

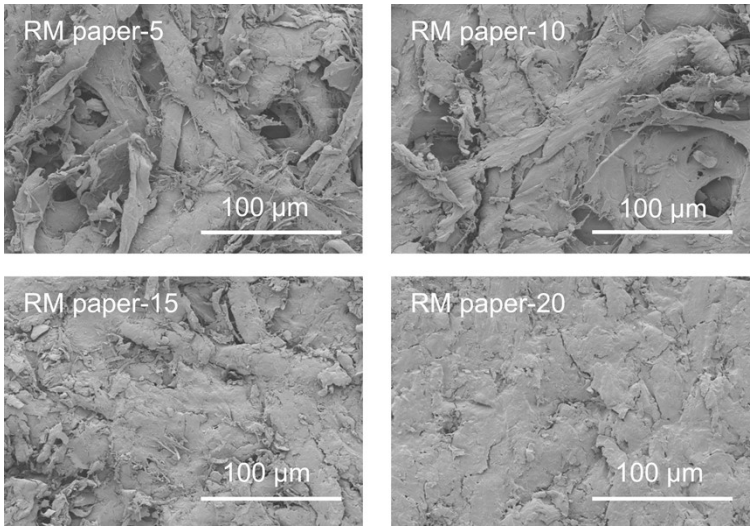

Figure S14. SEM images of RM paper after wear. With the increase of RM content, the structure of RM paper becomes denser and the fiber is wrapped by RM to prevent wear.

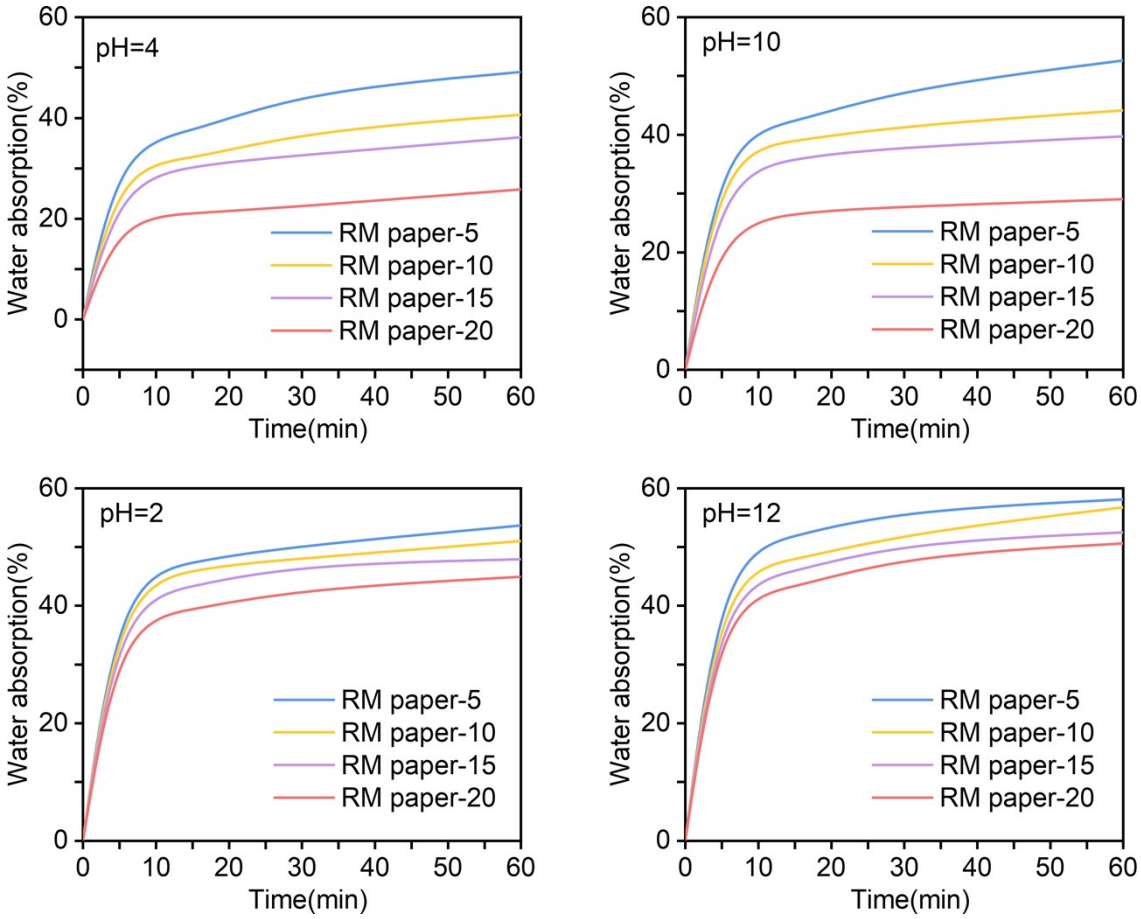

Figure S15. Acid and alkali resistance of RM paper.

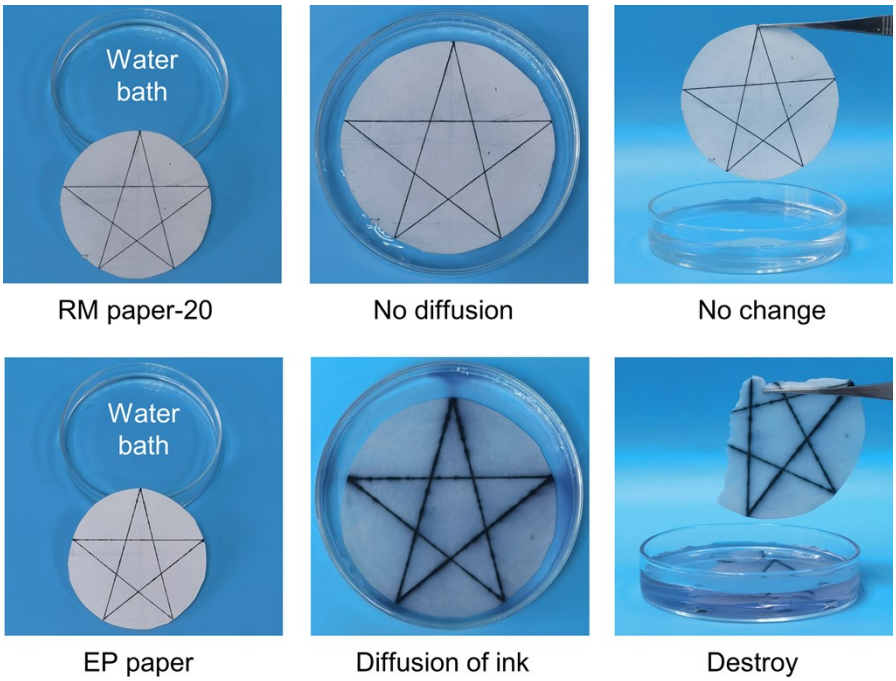

Figure S16. Printability of RM paper-20 and EP paper. The excellent water-resistance of the RM paper-20 prevents the penetration of water to protect the pattern on its surface, while the

high hydrophilicity of EP paper results in the complete destruction of both its structure and surface pattern.

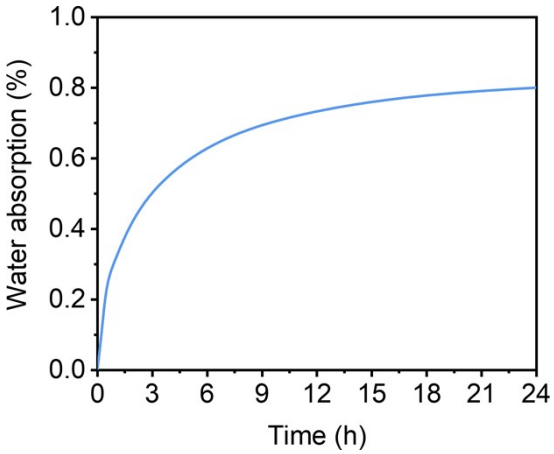

Figure S17. Water absorption of highly cross-linked polymers formed by RM polymerization.

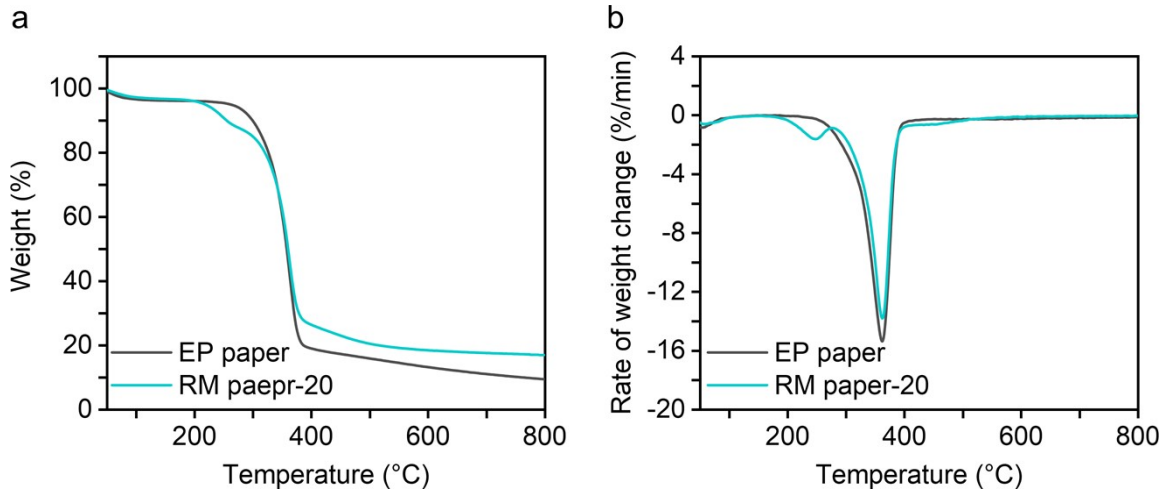

Figure S18. Thermal stability. TG a) and DTG b) curves of EP paper and RM paper-20 at a heating rate of 10 ℃·min^{-1} in N_2.

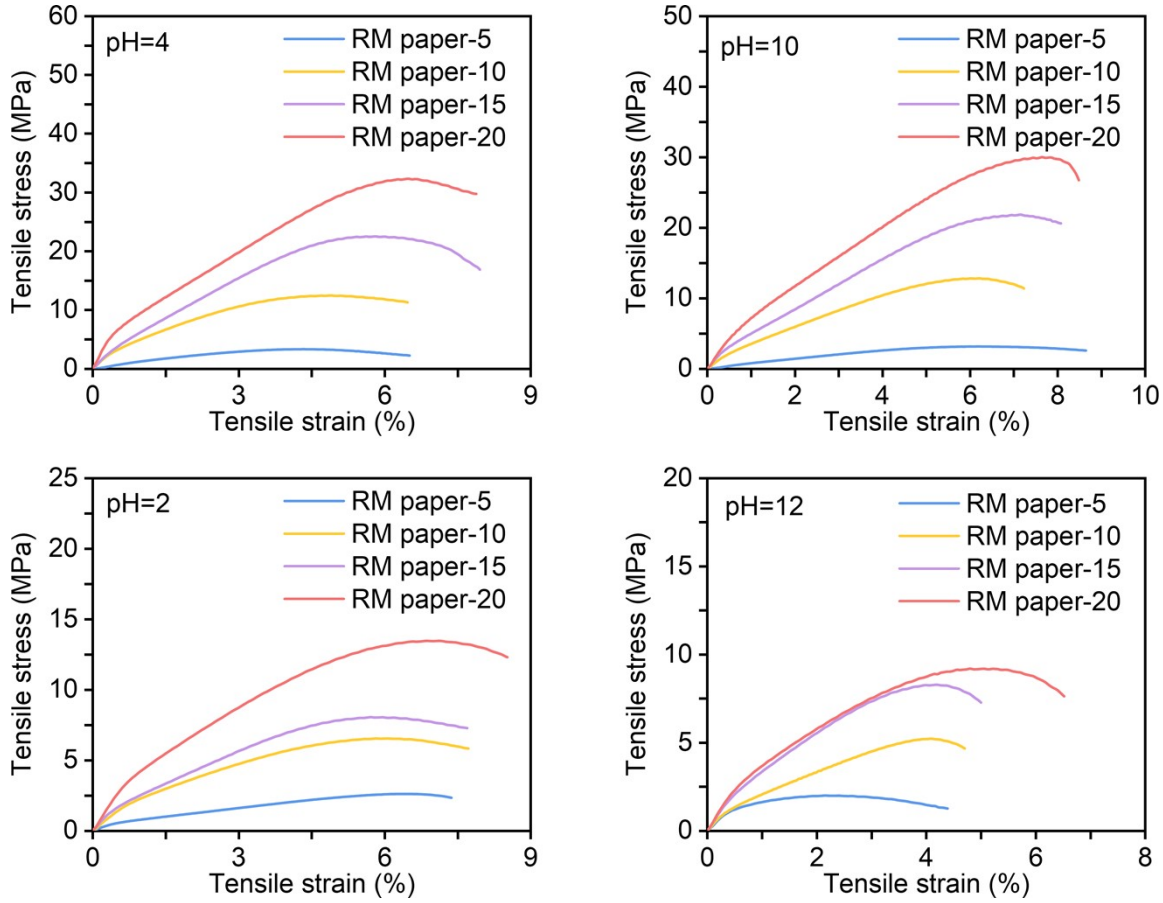

Figure S19. Mechanical properties of RM paper after soaking in acid and alkali solution.

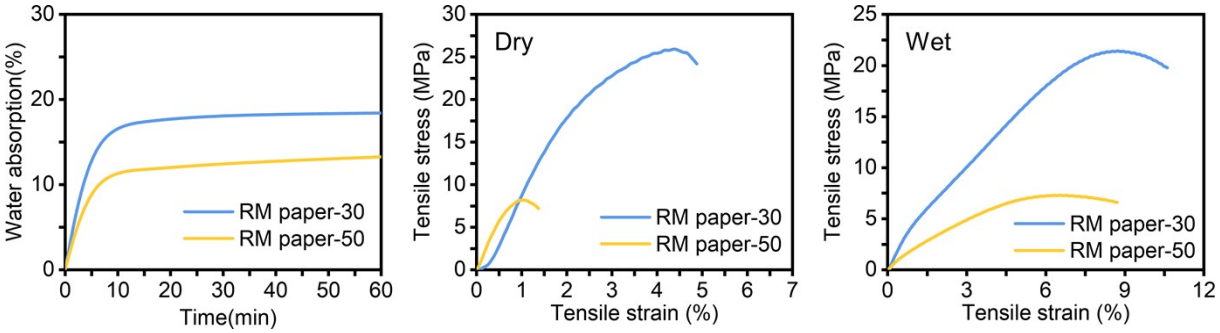

Figure S20. Water resistance and mechanical properties of RM paper-30 and RM paper-50.

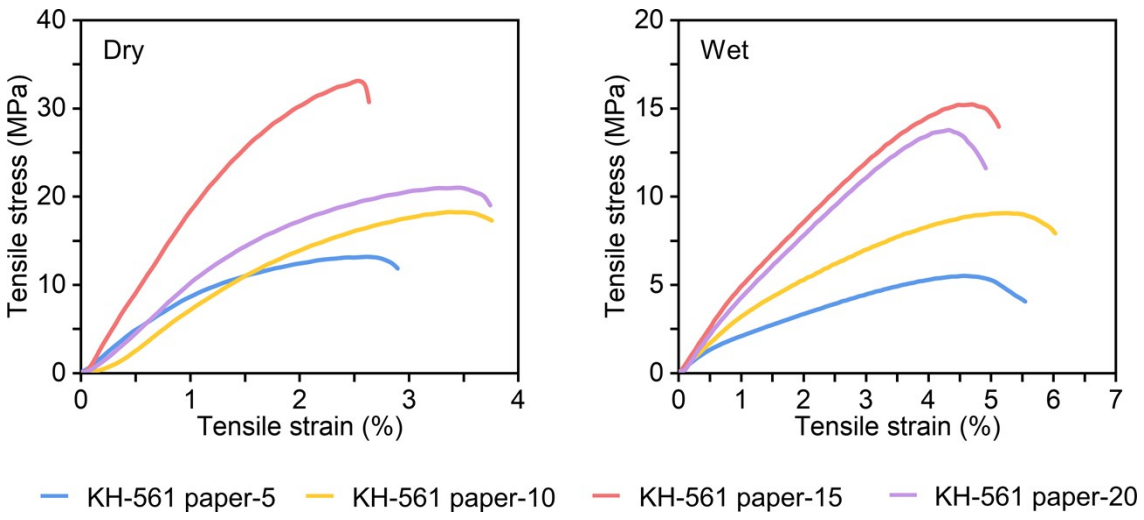

Figure S21. Mechanical properties of KH-561 grafted cellulose paper.

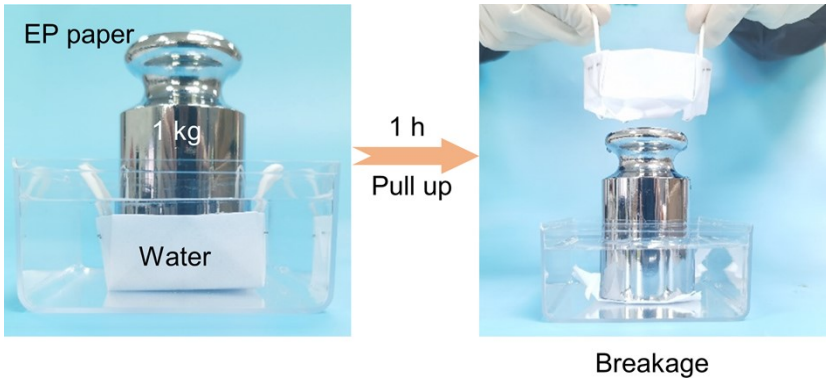

Figure S22. Mechanical properties of EP paper. The permeation of water destroys the hydrogen bonds between cellulose, which reduces the mechanical properties of the packing bag.

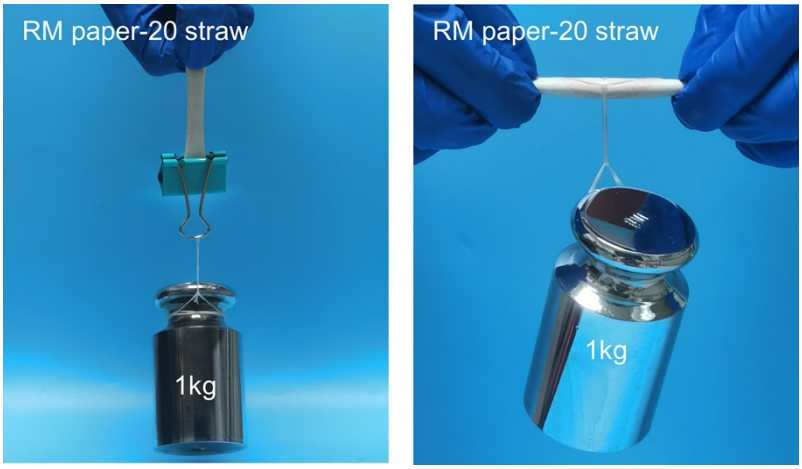

Figure S23. Mechanical properties of RM paper-20 straw after soaking for 240 min. The excellent water-resistance of RM paper-20 straw makes it difficult for water to penetrate, so it

still maintains high mechanical properties.

Figure S24. RM paper-20 straws are soaked in different drinks. RM paper-20 straws also show excellent liquid resistance for different drinks.

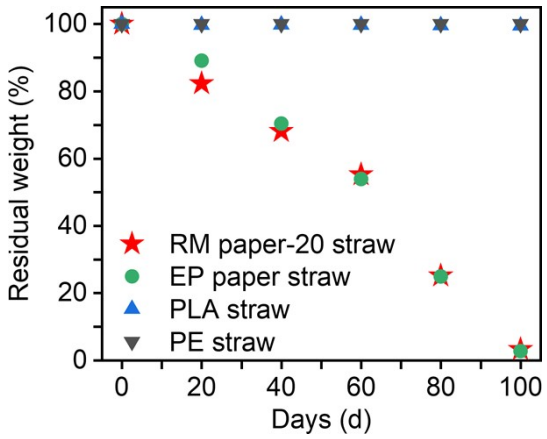

Figure S25. The weight loss curve of different straws. The degradation rates of RM paper-20 and EP paper are similar, while plastic straws have almost no degradable within 100 days.

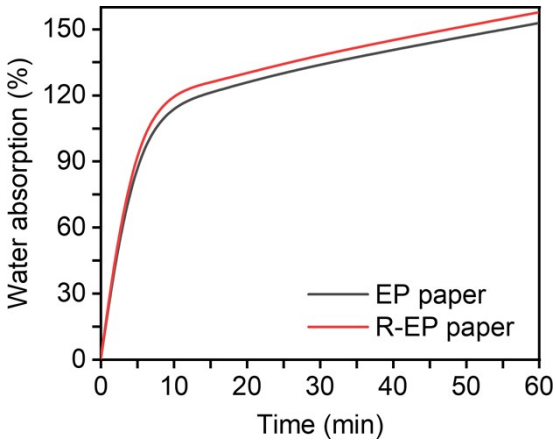

Figure S26. Water absorption of EP paper and R-EP paper. The water absorption curves of EP paper and R-EP paper are similar, which confirms the successful removal of RM.

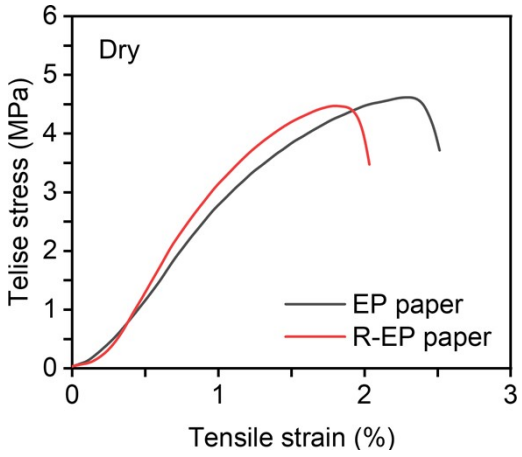

Figure S27. Tensile strength of EP paper and R-EP paper. The tensile strength of R-EP paper is close to that of EP paper, which further confirms the successful removal of RM.

Table S1. Performance comparison

References	Materials	Raw materials	Degradability	Cost	Tensile strength	Water absorption
This work	RM paper-20	Biomass	~100 days	~$1640 ton^{-1} a)	~47.8 MPa	~19.2%
[4]	Commercial paper	Biomass	~100 days	~$1200 ton^{-1} b)	~20 MPa	~126.3%
[5]	PE plastic	Petrochemical	>200 years	~$1500 ton^{-1} b)	~10.7 MPa	<1%
[6]	PLA plastic	Biomass	~3 years	>$7000 ton^{-1} b)	~46.7 MPa	<1%

a) In this work, the cost of materials mainly includes production costs. The cost of RM paper-20 is estimated based on the market price of raw materials. The price of fully hydrogenated rosin is about \$1950 ton^{-1}, that of KH-561 is about \$10000 ton^{-1}, and that of EP paper is about \$640 ton^{-1}. The mass ration of fully hydrogenated rosin to KH-561 in RM is 1.1:1. In RM paper-20, RM accounts for 20wt% and EP paper accounts for 80wt%. It is calculated that the production cost of RM is about \$5800 ton^{-1} and that of RM paper-20 is about \$1640 ton^{-1}.

b) The cost of other materials is calculated based on the industry's market intelligence and reported data.

Supplementary References

1 Q. Li, X. Huang, H. Liu, S. Shang, Z. Song and J. Song, *ACS Sustainable Chem. Eng.*, 2017, **5**, 10002-10010.

2 X. Yang, Z. Jiang, H. Liu, H. Zhang, X. Xu, S. Shang and Z. Song, *Polym. Degrad. Stab.*, 2021, **183**, 109422.

3 S. Wang, S. Wang, M. Shen, X. Xu, H. Liu, D. Wang, H. Wang and S. Shang, *ACS Sustainable Chem. Eng.*, 2021, **9**, 8623-8634.

4 C. Liu, P. Luan, Q. Li, Z. Cheng, X. Sun, D. Cao and H. Zhu, *Matter*, 2020, **3**, 2066-2079.

5 K. Kamau-Devers and S. A. Miller, *The International J. Life Cycle Assess.*, 2020, **25**, 1145-1159.

6 M. Kumar, S. Mohanty, S. K. Nayak and M. Rahail Parvaiz, *Bioresour. Technol.*, 2010, **101**, 8406-8415.